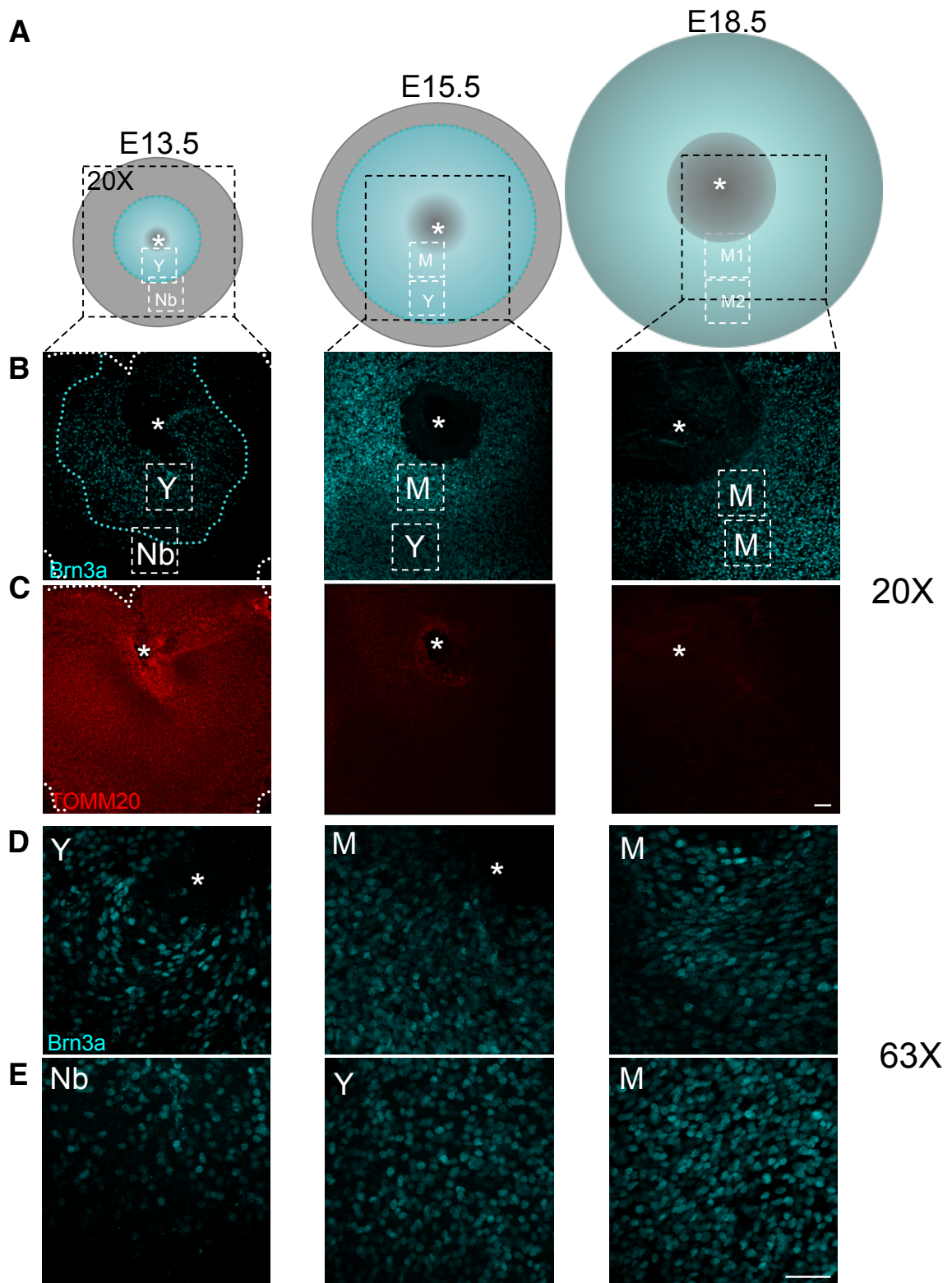


## Appendix Figures from Esteban-Martínez et. al

Programmed mitophagy is essential for the glycolytic switch during cell differentiation

### Table of contents

Appendix Figure S1 .....	Page 2
Appendix Figure S2 .....	Page 3
Appendix Figure S3 .....	Page 4
Appendix Figure S4 .....	Page 5
Appendix Figure S5 .....	Page 6
Appendix Figure S6 .....	Page 7
Appendix Figure S7 .....	Page 8

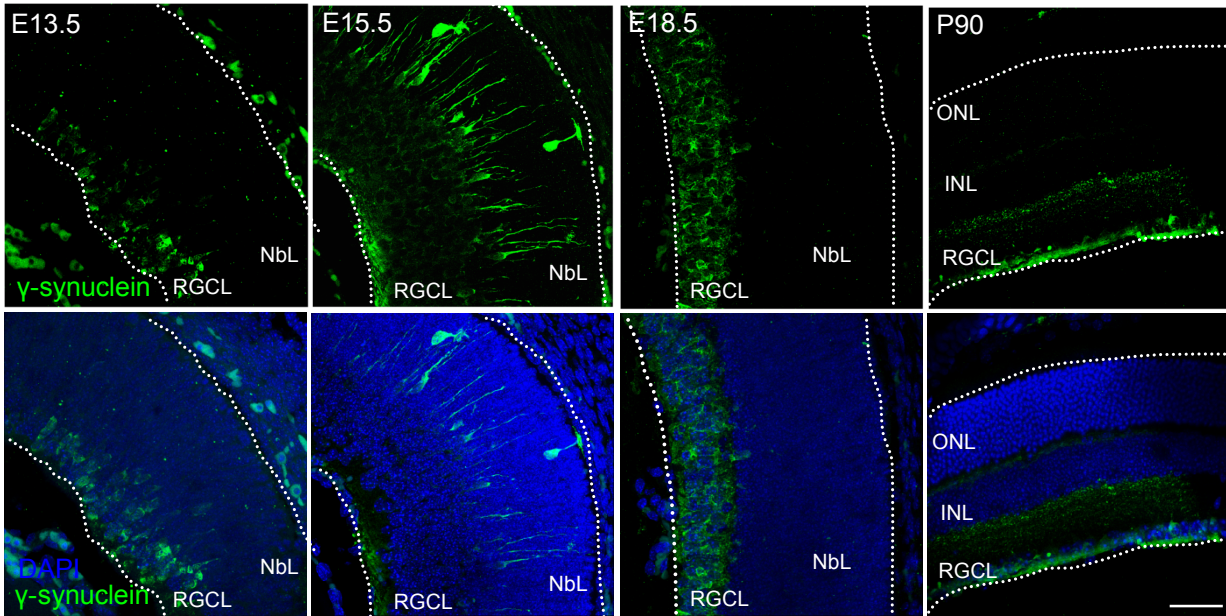


**Appendix Figure S1. RGC differentiation follows a central to peripheral gradient in the mouse embryonic retina.**

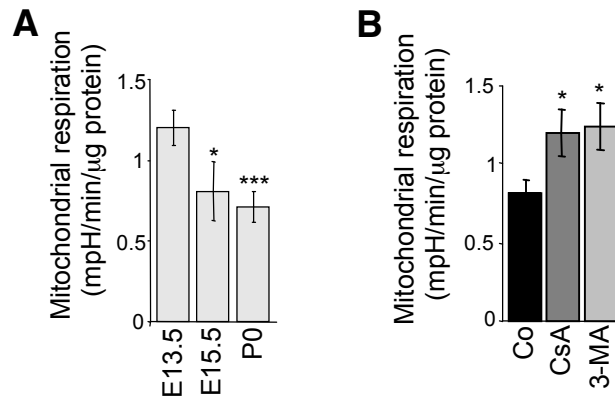
**A.** Drawings representing the mouse embryonic retina at E13.5, E15.5, and E18.5. Differentiation of RGCs (depicted in cyan) begins next to the optic nerve (white asterisk in grey background) and expands from the centre to the periphery of the retina, reaching the borders of the retina at E18.5. Y, young RGCs; Nb, neuroblast; M, mature RGCs.

**B-C.** Photomicrographs (20x magnification) of area depicted with black dashed lines in A, showing Brn3a (B, cyan) and TOMM20 (C, red) immunostaining.

**D-E.** Photomicrographs (63x magnification) of the areas depicted with white dashed lines in A. Note that the images in E are the same as those shown in Figure 1A.



**Appendix Figure S2. Progression of retinal ganglion cell (RGC) differentiation with  $\gamma$ -synuclein labelling.**  $\gamma$ -synuclein (green) immunostaining of RGCs in mouse retinal sections at the indicated developmental stages. DAPI-stained nuclei are shown in blue. Scale bar, 50  $\mu$ m.

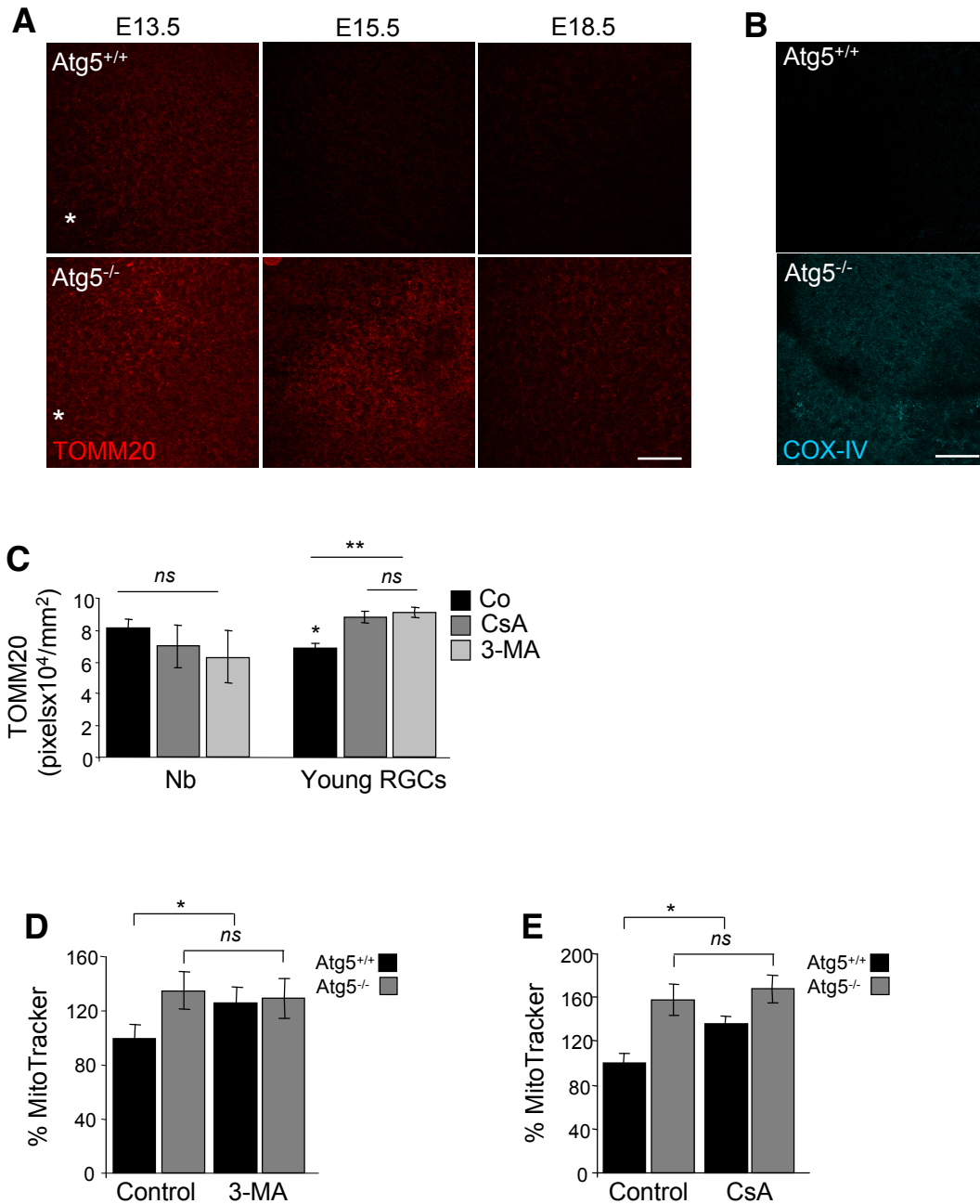


**Appendix Figure S3. Mitochondrial respiration during retinal development and following inhibition of autophagy or mitophagy**

**A.** Mitochondrial respiration in embryonic retinas at the indicated developmental stages ( $n = 19$ – $49$  pools of retinas per group).

**B.** Mitochondrial respiration in E15.5 retinas incubated for 6 h in the presence of 3-MA or CsA ( $n = 15$ – $19$  pools of 2 retinas per group).

Data information: Data are presented as mean  $\pm$  SEM. \* $P < 0.05$ ; \*\*\* $P < 0.001$  (Mann-Whitney  $U$ -test).



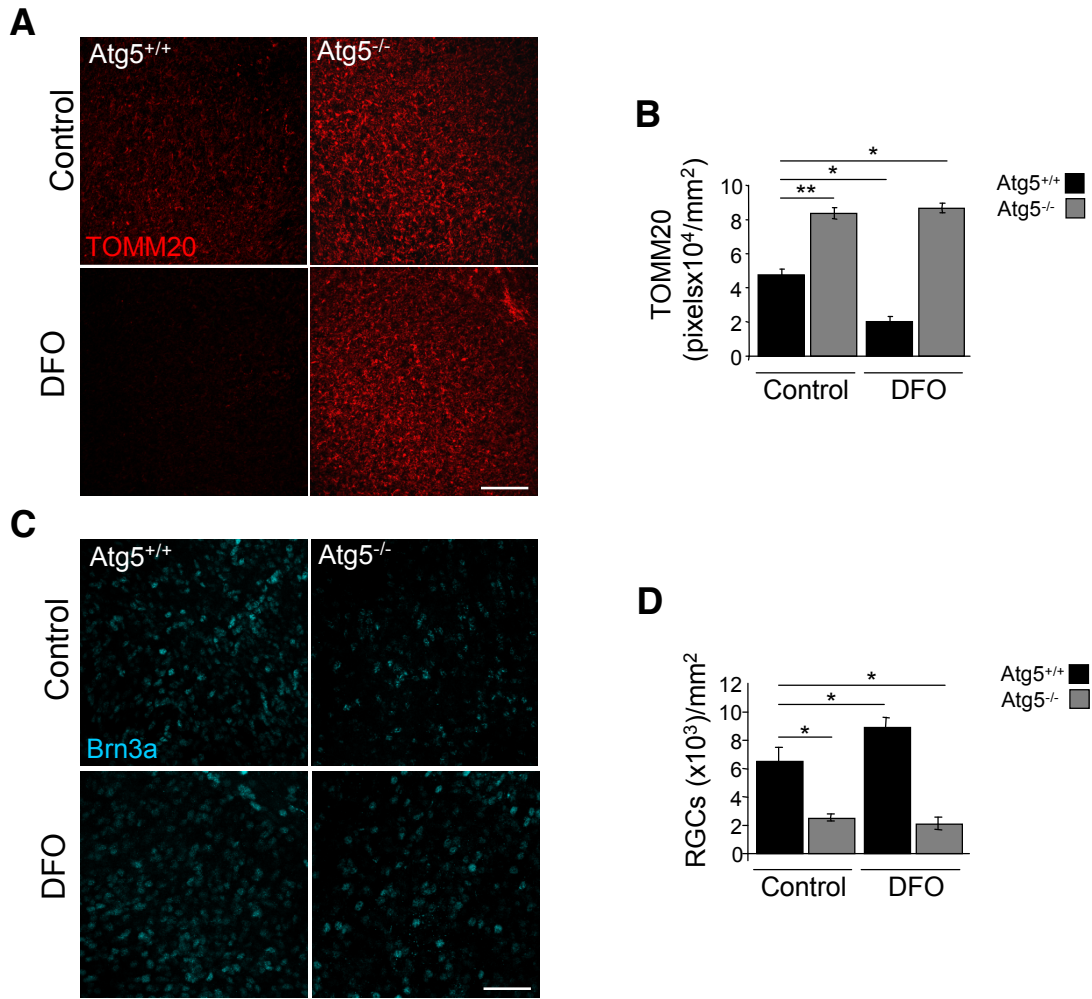
**Appendix Figure S4. Increased mitochondrial levels in Atg5-deficient retinas.**

**A.** TOMM20 immunostaining in wild-type (Atg5<sup>+/+</sup>) and Atg5-deficient (Atg5<sup>-/-</sup>) retinal wholemounts corresponding to the indicated embryonic stages. Scale bar, 50  $\mu$ m.

**B.** COX-IV immunostaining in E15.5 wild-type (Atg5<sup>+/+</sup>) and Atg5-deficient (Atg5<sup>-/-</sup>) retinal wholemounts. Scale bar, 50  $\mu$ m.

**C.** Quantification of TOMM20 immunostaining in neuroblasts (Nb) and young RGCs in retinas incubated for 6 h with 3-MA or CsA ( $n = 4-6$  retinas per group). Data are presented as mean  $\pm$  SEM. \* $P < 0.05$ ; \*\* $P < 0.01$  (Mann-Whitney  $U$ -test).

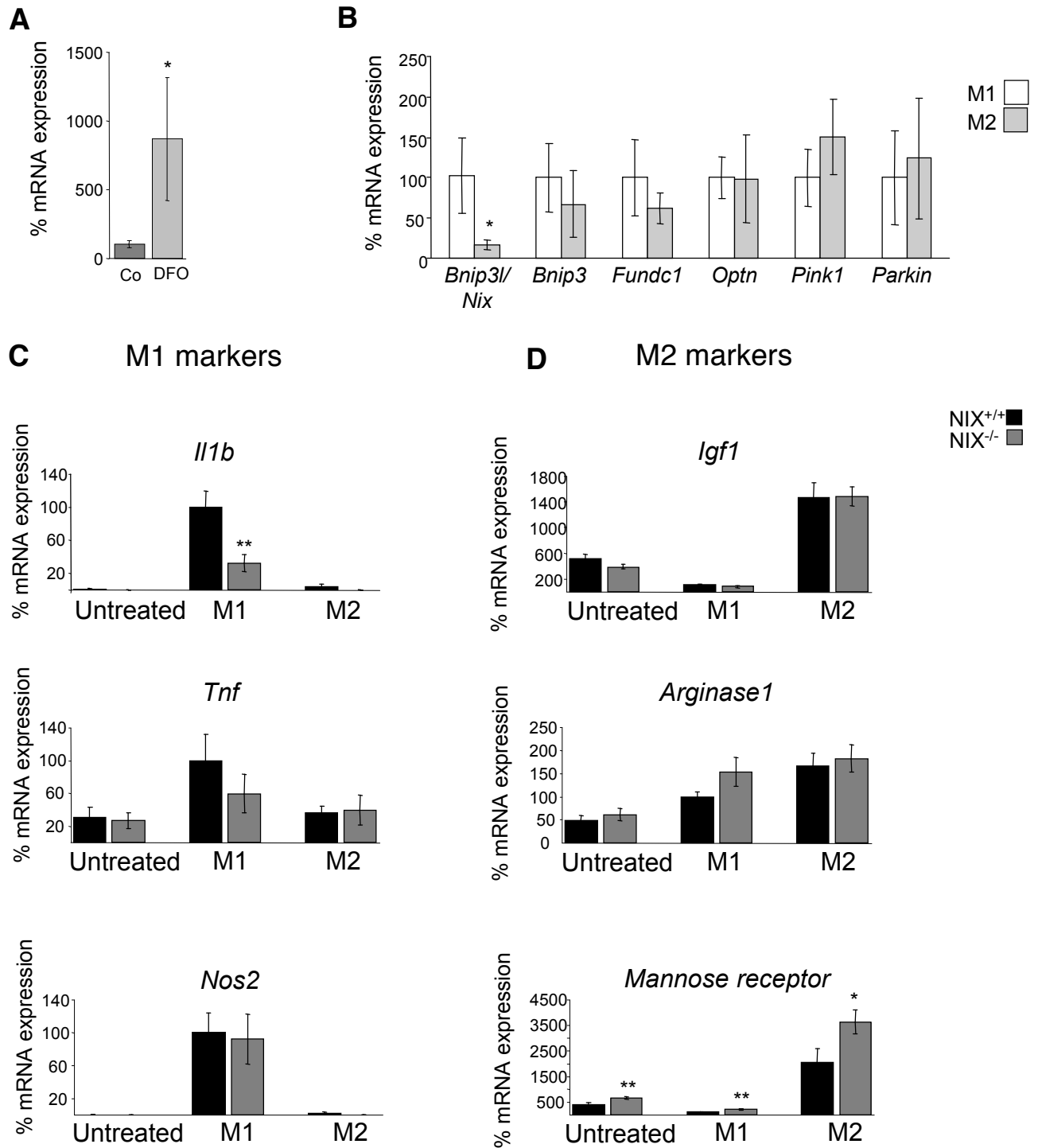
**D, E.** Percentage mean fluorescence intensity (% MitoTracker) in E15.5 wild-type (Atg5<sup>+/+</sup>) and Atg5-deficient (Atg5<sup>-/-</sup>) retinas incubated in the absence or presence of 3-MA (**E**) ( $n = 9-16$  retinas per group) or CsA (**F**) ( $n = 5-7$  retinas per group). Data are presented as mean  $\pm$  SEM. \* $P < 0.05$  (Mann-Whitney  $U$ -test).



**Appendix Figure S5. Hypoxia is upstream of mitophagy**

**A, B.** TOMM20 immunostaining (**A**) and corresponding quantification (**B**) of retinal flatmounts from wild-type (Atg5<sup>+/+</sup>) and Atg5-deficient (Atg5<sup>-/-</sup>) mice (E15.5) in the absence or presence of the hypoxia inducer DFO (1 mM) ( $n = 4-6$  per group). Scale bar, 50  $\mu\text{m}$ . Data are presented as mean  $\pm$  SEM. \* $P < 0.05$ ; \*\* $P < 0.01$  (Mann-Whitney  $U$ -test).

**C, D.** Brn3a immunostaining (**C**) and corresponding quantification (**D**) in retinal flatmounts from wild-type (Atg5<sup>+/+</sup>) and Atg5-deficient (Atg5<sup>-/-</sup>) mice (E15.5) in the absence or presence of the hypoxia inducer DFO (1 mM) ( $n = 4-9$  per group). Scale bar, 50  $\mu\text{m}$ . Data are presented as mean  $\pm$  SEM. \* $P < 0.05$  (Mann-Whitney  $U$ -test).



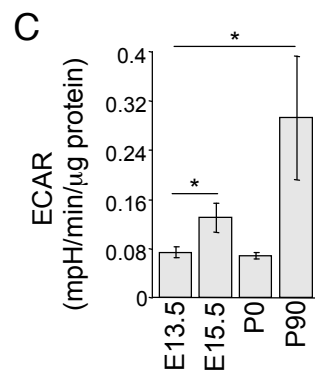
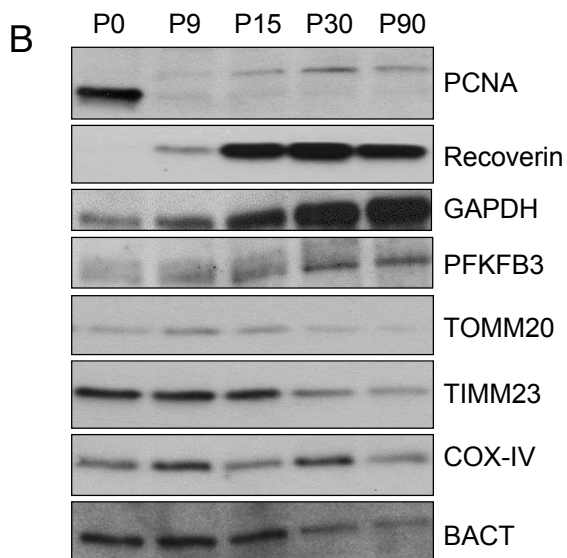
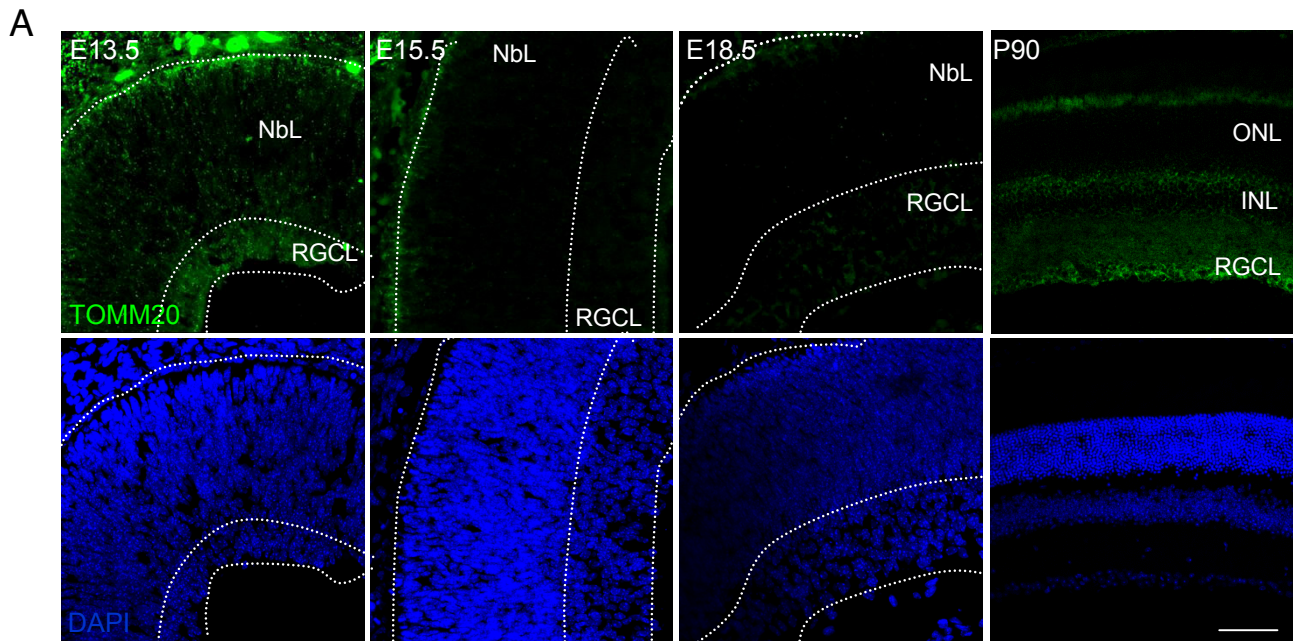
**Appendix Figure S6. M1 responses are decreased in NIX-deficient mice.**

**A.** mRNA expression of *Bnip3/Nix* in retinas treated with DFO.  $n = 3-8$  retinas per group). Data are presented as mean  $\pm$  SEM. \* $P < 0.05$  (Mann-Whitney *U*-test).

**B.** mRNA expression of the indicated genes in M1 versus M2 macrophages ( $n = 5-7$  per group). Data are presented as mean  $\pm$  SEM. \* $P < 0.05$  (Mann-Whitney *U*-test).

**C.** mRNA expression of the M1 markers in untreated M1, and M2 macrophages from wild-type (NIX<sup>+/+</sup>) and NIX-deficient (NIX<sup>-/-</sup>) mice ( $n = 7-8$  per group). Data are presented as mean  $\pm$  SEM. \*\* $P < 0.01$  (Mann-Whitney *U*-test).

**D.** mRNA expression of M2 markers in untreated M1, and M2 macrophages from wild-type (NIX<sup>+/+</sup>) and NIX-deficient (NIX<sup>-/-</sup>) mice ( $n = 7-8$  per group). Data are presented as mean  $\pm$  SEM. \* $P < 0.05$ ; \*\* $P < 0.01$  (Mann-Whitney *U*-test).



**Appendix Figure S7. Mitochondrial content and glycolysis during postnatal development of the retina.**

**A.** TOMM20 (green) immunostaining in mouse retinal sections at the indicated developmental stages. DAPI-stained nuclei are shown in blue. NbL, neuroblast layer; RGCL, retinal ganglion cell layer, INL, inner nuclear layer, ONL, outer nuclear layer. Scale bar, 75  $\mu$ m.

**B.** Immunoblotting of retinas at different embryonic stages for proliferative cells (PCNA-positive), photoreceptor cells (recoverin-positive), glycolytic enzymes (GAPDH and PFKFB3), and mitochondrial proteins (TOMM20, TIMM23, and COX-IV).

**C.** Extracellular acidification rate (ECAR) in embryonic and adult retinas at the indicated developmental stages ( $n = 19$ – $49$  pools of retinas per group). Data are presented as mean  $\pm$  SEM. \* $P < 0.05$  (Mann-Whitney  $U$ -test).